Intelligent Control of Ackermann Autonomous Vehicles via Neural Network-Enhanced Fuzzy-PID: A Simscape Multibody-Based Simulation Study

Thanh-Ha Vo [1], Thi-Thuy Chu [2], Quang-Vinh Vo [3], and Hong-Quang Nguyen [4,*]

[1] Faculty of Electrical and Electronic Engineering, University of Transport and Communications, Hanoi, Vietnam
[2] Faculty of Electrical Engineering and Automation,
University of Economics-Technology for Industries, Hanoi, Vietnam
[3] Faculty of Mechanical, Automotive and Civil Engineering, Electric Power University, Hanoi, Vietnam
[4] Faculty of Mechanical, Electrical, Electronics Technology,
Thai Nguyen University of Technology, Thai Nguyen, Vietnam
Email: vothanhha.ktd@utc.edu.vn (T.H.V.); ctthuy@uneti.edu.vn (T.T.C.); vinhvq@epu.edu.vn (Q.V.V.);
quang.nguyenhong@tnut.edu.vn (H.Q.N.)
*Corresponding author

***Abstract*—To adapt to these new conditions, this movement towards safe, accurate, and high-speed (ease of operation) control for autonomous vehicles requires adaptive control strategies that adjust for nonlinear dynamics and unpredictable operating conditions. This paper proposes an intelligent control framework for Ackermann-type automated vehicles based on a Neural Network-Optimized Fuzzy Proportional-Integral-Derivative (NN-FPID) controller to circumvent the shortcomings of traditional PID and fixed-rule Fuzzy-PID controllers. Using a lightweight neural network, the fuzzy membership functions and PID gains can be continuously and automatically updated based on the vehicle's steering error, velocity error, and lateral deviation. The Ackermann vehicle model is generated in Simscape Multibody, enabling simulation of kinematic and dynamic behavior with realistic components for vehicle control. Compared to the control controller, the new NN-FPID controller reduces Root Mean Square Error (RMSE) for lateral tracking by 50–60%, overshoot by up to 65%, and settling time by approximately 55% across straight roads, turns, zigzags, bumps, and other road conditions. The average time per control step is less than 1 ms, supporting the deployment of this technique for real-time implementation in embedded autonomous driving systems.**

***Keywords*—fuzzy-Proportional–Integral–Derivative (PID), Neural Network-Optimized Fuzzy Proportional-Integral-Derivative (NN-FPID), Ackermann, autonomous vehicles**

I. Introduction

have driven the increased need for both adaptive and reliable control strategies to manage the nonlinear behavior of Ackermann-type vehicles in real-time and uncertain environments [1, 2]. Traditional techniques, including Proportional–Integral–Derivative (PID) PID, Linear Quadratic Regulator (LQR), Model Predictive Control (MPC), and sliding-mode controllers, have been extensively applied to lateral and longitudinal control [3–5]. MPC and Sliding-Mode Control (SMC) possess remarkable robustness and effective constraint handling, but their high computational cost, sensitivity to model accuracy, and reliance on precise system parameters may make them infeasible for low-cost embedded systems and real-time autonomous driving systems. On the contrary, the proposed Neural Network-Optimized Fuzzy Proportional-Integral-Derivative (NN-FPID) controller offers a good trade-off among adaptability, interpretability, and computational efficiency, making it well-suited for real-time implementation on resource-constrained hardware.

To the authors' knowledge, no other research has combined real-time neural network adjustments with fuzzy-PID control and tested them simultaneously on a detailed Simscape Multibody Ackermann vehicle model.

Although PID is valued for its simplicity, it degrades in performance when operating conditions change, whereas MPC offers high accuracy at the cost of excessive computational complexity [6, 7]. In response, Fuzzy-PID control has gained popularity as a practical compromise, merging the interpretability of fuzzy logic with the robustness of PID control [8–10]. However, most existing hybrids rely on manual tuning of fuzzy membership functions and rule bases, thereby limiting adaptability to varying speeds, curvatures, and tire conditions [11, 12]. Some efforts on Adaptive Fuzzy-PID (AFPID) have

Manuscript received November 18, 2025; revised December 9, 2025; accepted March 24, 2026; July 10, 2026.

demonstrated improved performance, yet their real-time applicability to Ackermann steering systems remains limited [13]. Concurrently, data-driven techniques have begun to influence vehicle control. Neural Networks (NNs) and Adaptive Neuro Fuzzy Inference Systems (ANFIS) have demonstrated success in disturbance estimation, trajectory planning, and control optimization [14–17]. Yet the literature lacks implementations that integrate NNs to auto-tune Fuzzy-PID controllers in real time for Ackermann platforms.

This work addresses that gap by introducing an NN-FPID controller tailored for Ackermann-type autonomous vehicles.

This paper makes the following key contributions:

- Vehicle Control Validation: The performance of a simulation of the control system is evaluated by a special Simscape Multibody Ackermann model of a vehicle to be able to represent the true limits, weight effects, and tyre-road interactions, and used as a vehicle testing ground for autonomous vehicle control.
- A new self-driving-style, dual-loop steering and speed control system by a modern model based on NN fuzzy-PID control becomes more precise, adjusts better to disturbances, and does not rely on randomness.
- A neural network is employed to automatically update fuzzy membership functions and PID gains in response to variations in road grip and vehicle weight, but without relying on input noise.

Quantitative performance improvements concretely real-time feasibility: The simulation of tests under all driving scenarios demonstrates that the NN-Fuzzy-PID controller can achieve measurable improvements such as up to a 50–60% decrease in lateral RMSE, 65% or more reduction in overshoot or approximately 55% less settling time compared with the standard controllers, and an average recovery time of less than 1 ms per control step of the controller in real time.

The performance of the systems was evaluated by simulating straight, curved, and zigzag paths at various speeds, friction levels, and disturbances, and performance was shown to improve from moment to moment.

The rest of the paper presents Ackermann's car model in Section II. The controller designs are presented in Section III. Section IV describes the simulation's uses and how it will be scored using metrics; Section V presents findings; Section VI outlines future research directions.

II. Kinematic and Dynamic Modelling Using Simscape Multibody

A. Kinematic Model of the Ackermann Steering

Ackermann steering uses bicycle or four-wheel models in which the wheels share a common Instantaneous Center of Rotation (ICR), preventing lateral slip during low-speed maneuvering and trajectory tracking. Fig. 1 shows wheelbase L, track width t, and inner δ_i and outer δ_0 steering angles. The ICR is on the extended rear axle at R. Vehicle body coordinates X_c, Y_c, θ_c define kinematic equations, leading to state-space formulation in Eqs. (1)–(3).

Ackermann steering geometry ensures that during turning, all wheels trace circular paths with a common center, minimizing tire slip. For a vehicle with wheelbase L, track width t, and steering angles, δ_{in} δ_{0ut} the geometric constraint is given by Eq (1):

$$tan(\delta_{in}) = \frac{L}{R-\frac{t}{2}};\ \tan(\delta_{0ut}) = \frac{L}{R+\frac{t}{2}} \tag{1}$$

where R is the turning radius. For controller design, the system is often reduced to the bicycle model, described by Eq. (2):

$$\begin{cases} \dot{x} = vcos\theta \\ \dot{y} = vcos\theta \\ \dot{\theta} = \frac{v}{L}cos\theta \end{cases} \tag{2}$$

where (x, y) is the vehicle position, v is the longitudinal velocity, and θ is the equivalent steering angle.

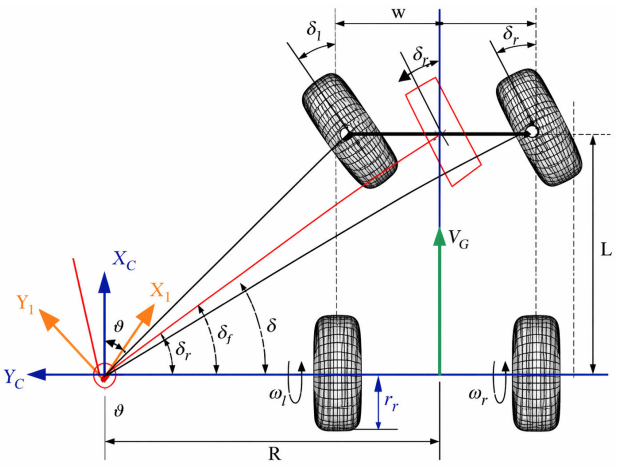

Fig. 1. Ackermann steering geometry.

For modeling consistency and fair performance evaluation, the same set of vehicle parameters is employed in the analytical formulation and the Simscape.

Multibody model. The main physical and geometric parameters of the Ackermann vehicle are listed in Table I.

TABLE I. Vehicle Parameters

Parameter	Value
Mass	1200 kg
Wheelbase	2.6 m
Track width	1.5 m
Max steering	±30°

B. Dynamic Model with Tire-Road Interaction

To capture realistic behavior, the dynamic model accounts for inertia, yaw motion, and tire-road interaction. The planar dynamics are expressed as Eqs. (3) and (4):

$$m(\dot{v}_x + v_y r) = F_{xf} + F_{xr} \tag{3}$$

$$I_z \dot{r} = l_f F_{yf} - l_r F_{yr} \quad (4)$$

where: m is vehicle mass; v_x, v_y are longitudinal and lateral velocities; r is yaw rate; I_z is yaw moment of inertia; l_f, l_r are distances from the center of gravity to the front and rear axles; F_{yf}, F_{yr} are lateral tire forces.

The tire forces are modeled as Eq. (5):

$$F_y = -C_\alpha \alpha \quad (5)$$

with C_α is the cornering stiffness coefficient and α the slip angle of the tire. This formulation enables the vehicle model to represent both kinematic constraints and lateral dynamics under different maneuvering conditions, forming the basis for subsequent controller design.

C. Modeling Assumptions and Operating Conditions

In this work, several assumptions have been adopted to fa To enable control-focused modelling while recognising the basic dynamics of the vehicle. Various assumptions are applied in this work. These assumptions include:

- The body of the vehicle is treated as a rigid body with no consideration of structural flexibility.
- The forces caused by tires are represented with a linear tire model, suitable for the small slip angles found in low- to medium-speed autonomous driving.
- Vehicle operation is limited to low and medium speeds, in which case, lateral load transfer and high-frequency nonlinear effects are of less significance.
- Roll and pitch dynamics are ignored, and motion is assumed to be planar, prioritizing the dynamics of the form through longitudinal, lateral, and yaw operations.

Such assumptions, which are often used in autonomous vehicle control research, offer a good compromise between model simplicity and simulation accuracy—most especially when verified with high-fidelity tools like Simscape Multibody.

D. High-Fidelity Implementation in Simscape Multibody

The compact and computationally efficient kinematic and dynamic equations described in Sections II.A and II.B, however, help to guide the theoretical design of controllers. They neglect vital nonlinear and structural phenomena encountered in real life. Thus, the higher-fidelity Simscape Multibody model in Section II.C supplements these formulations, enabling validation and realistic simulations of Ackermann vehicle dynamics. Fig. 2 provides an overview of the modelling workflow and its five core components: (1) chassis and steering linkage construction, (2) actuation and kinematic reference definitions, (3) tire-road interactions modelling, (4) PID or Fuzzy-PID controllers integration, and (5) simulation and validation. The resulting pipeline allows for consistent representation of both mechanical dynamics and control algorithms.

As a result of the Simscape Multibody modeling steps, the Ackermann vehicle was represented through three main subsystems: the chassis (Fig. 3), the front suspension and wheel assembly (Fig. 4), and the rear suspension and wheel assembly (Fig. 5). These models form the physical foundation for subsequent controller integration and dynamic simulation.

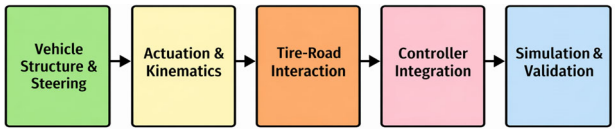

Fig. 2. Block diagram of the modeling workflow in Simscape Multibody for the Ackermann vehicle, consisting of five main steps.

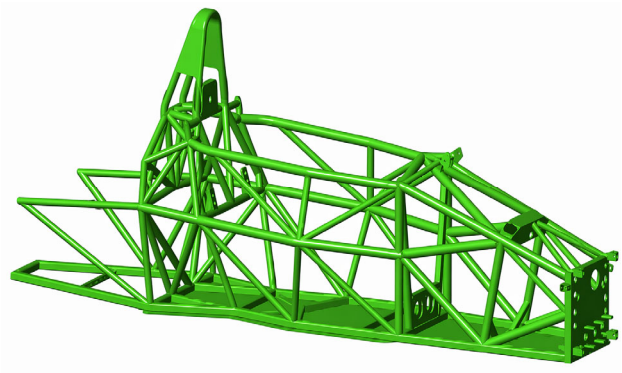

Fig. 3. Simscape Multibody chassis model of the Ackermann vehicle.

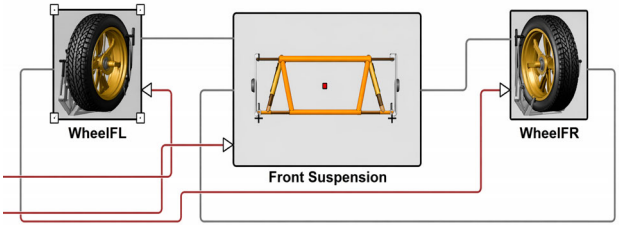

Fig. 4. Front suspension and wheel subsystem of the Ackermann vehicle.

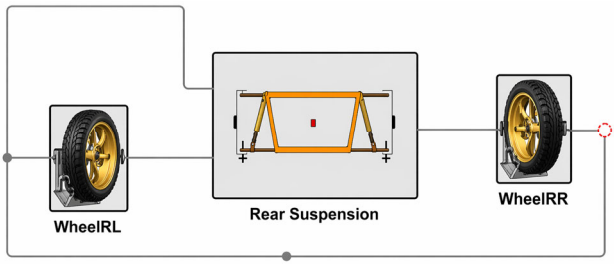

Fig. 5. Rear suspension and wheel subsystem of the Ackermann vehicle.

The accuracy of the Simscape Multibody implementation was validated through simulation. Fig. 6 shows the 3D vehicle model in Mechanics Explorer, and Fig. 7 compares its outputs with those from the coordinate-based formulation. The close agreement in velocity, friction force, and torque confirms the reliability of the multibody approach.

Figs. 6 and 7 prove the Ackermann model of the vehicle in Simscape Multibody. The 3D model (Fig. 6) accurately captures the chassis, suspension, and wheel behavior. The comparison (Fig. 7) between the coordinate-based and multibody models shows a strong correlation, thereby validating the accuracy and utility of Simscape for detecting friction, inertia, and load transfer. The outputs of the Simscape Multibody model are further compared with

those of the analytical kinematic model to quantitatively validate the multibody implementation. The resulting RMS error is lower than 3.2% for longitudinal velocity and 4.5% for yaw rate, demonstrating the strong numerical agreement of the two models.

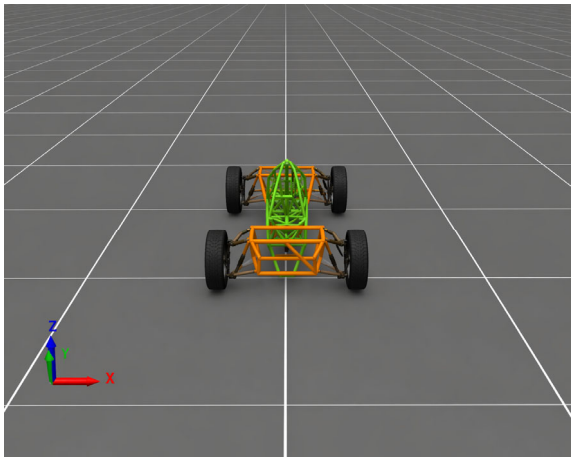

Fig. 6. 3D visualization of the Ackermann vehicle model in Simscape Multibody.

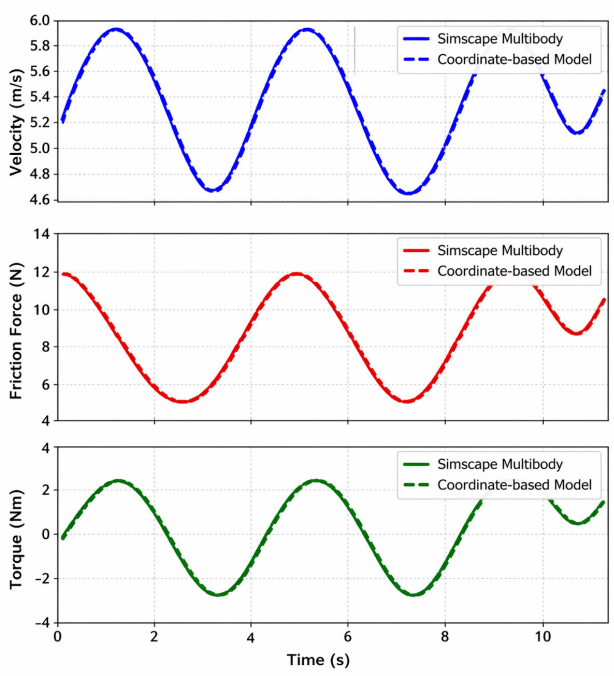

Fig.7. Comparison of velocity, friction, and torque between the coordinate-based and Simscape Multibody models.

III. Dual-Loop NN-Fuzzy-PID Controller Design

Although the controller is validated on an Ackermann steering vehicle, its structure is not restricted to this configuration. The NN-Fuzzy-PID design is developed based on a general nonlinear state-space formulation and adaptive gain tuning driven by measurable tracking errors. Therefore, the proposed framework can be extended to other ground vehicle architectures, such as four-wheel steering systems or differential-drive platforms, with appropriate modifications in the kinematic mapping stage.

A. Control Architecture Overview

The proposed controller combines Fuzzy logic and a Neural Network (NN) to enhance PID control in both steering (lateral) and velocity (longitudinal) regulation.

- The fuzzy logic role provides adaptive gain scheduling by mapping the error e and the error change Δe into corrections $\Delta K_p, \Delta K_i, \Delta K_d$, using a rule base (IF-THEN rules with linguistic labels NB, NS, Z, PS, PB). This layer ensures that the controller reacts appropriately to small and large deviations, improving robustness to nonlinearities.
- The neural network role continuously tunes the fuzzy membership functions and rule weights online, based on performance feedback. Unlike static fuzzy rules, the NN updates the fuzzy inference system to minimize a performance index *J*. This learning capability enables long-term adaptability to varying road friction, vehicle load, and dynamic conditions.

The PID role ensures stability and well-known control dynamics, with gains dynamically adjusted by the fuzzy-NN layers as Eq (6):

$$\begin{cases} K_p^* = K_p + \Delta K_p \\ K_i^* = K_i + \Delta K_i \\ K_d^* = K_d + \Delta K_d \end{cases} \quad (6)$$

The lateral and longitudinal control loops are designed independently from each other, but they are interlocked with vehicle dynamics. Specifically, vehicle speed directly affects lateral response; steering behavior modifies longitudinal behavior via tire force distribution. In this research, the coupling is implicitly accounted for using common state variables, neural network-based adaptive tuning of fuzzy-PID gains, and a very high-fidelity Simscape Multibody model that leverages the nonlinear characteristics of interaction. The stability of the coupled system is verified through simulation under varying speeds, disturbances, and parameter uncertainties, where all state variables remain bounded and converge smoothly. In this work, neither a formal theoretical analysis of coupling and stability is provided; the study on the latter will be developed in following work.

B. In the Lateral Control Loop

The steering loop minimizes lateral deviation and heading error relative to the reference path. A feedforward term based on road curvature is combined with feedback corrections by Eq. (7):

$$\delta_{ref} = \arctan(L_K) + K_1 e_\varphi + K_2 \arctan\left(\frac{e_y}{\epsilon + v_x}\right) \quad (7)$$

where L_K is the wheelbase; K_r is the reference curvature, e_y is the lateral error, and e_φ the heading error, the ϵ is regularization term ($\epsilon = 0.1 \div 1$); v_x is longitudinal velocity of the vehicle.

The NN-Fuzzy-PID controller regulates the steering actuator by adaptively tuning PID gains K_p , K_i , K_d based on the error and its rate of change. This enhances stability

during large deviations and responsiveness near equilibrium.

C. Longitudinal Control Loop

The velocity loop maintains the desired longitudinal speed while compensating for nonlinear effects such as road-tire friction, inertia, and load transfer. The control error is defined as Eq. (8):

$$e_v = v_{ref} - v_x \tag{8}$$

with its derivative $\dot{e}_v$. The NN-Fuzzy-PID generates adaptive corrections to the PID gains, complemented by a feedforward term accounting for rolling resistance and aerodynamic drag as Eq. (9):

$$T_{ff} = m\dot{v}_{ref} + c_r 0.5\rho A v_x^2 \tag{9}$$

The final torque/throttle command is expressed as Eq. (10):

$$T_{cmd} = sat\left(K_p^* e_v\right) + K_i^* \int e_v dt + K_d^* \dot{e}_v + T_{ff}; [T_{min}, T_{max}] \tag{10}$$

D. Fuzzy Inference System and Rule Base

The NN-Fuzzy-PID controller employs a fuzzy inference system to adapt the PID gains in real time, as shown in Fig. 8.

The inputs are the control error e and its derivative Δe, and the outputs are incremental corrections. K_p, K_i, K_d, a seven-level fuzzy set (NB, NM, NS, Z, PS, PM, PB) is adopted to provide fine granularity and smooth adaptation. The rule base (Table II) maps combinations of e and Δe to gain adjustments, enabling fast response to large deviations and stability around the equilibrium. In this hybrid framework, the fuzzy logic layer provides interpretable, rule-based gain scheduling, while the neural network layer continuously adjusts membership functions and rule weights online. This ensures that the controller not only reacts effectively to instantaneous errors but also adapts its behavior to long-term variations in road friction, load transfer, and vehicle dynamics. As a result, the NN-Fuzzy-PID achieves both robustness and adaptability beyond conventional PID or static fuzzy-PID schemes.

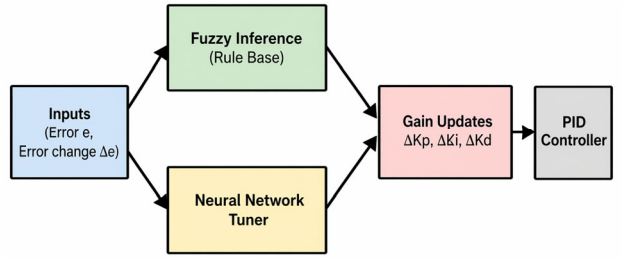

Fig. 8. Structure of NN-Fuzzy-PID tuning mechanism.

TABLE II. FUZZY RULE BASE FOR ADAPTIVE PID GAIN TUNING

Δe\e	NB	NM	NS	Z	PS	PM	PB
NB	↑↑Kp, ↓↓Ki, ↑↑Kd	↑↑Kp, ↓Ki, ↑Kd	↑Kp, ↓Ki	↑Kp	↑Kp, ↑Ki	↑Kp, ↑Ki, slight ↓Kd	moderate ↑Kp
NM	↑↑Kp, ↓Ki, ↑Kd	↑Kp, ↓Ki	↑Kp	↑Kp	↑Kp, ↑Ki	↑Kp, ↑Ki	↑Kp, ↑Ki, ↓Kd
NS	↑Kp, ↓Ki	↑Kp	↑Kp	stable	↑Kp	↑Kp, ↑Ki	↑Kp, ↑Ki, ↓Kd
Z	↑Kp	↑Kp	stable	no change	stable	↓Kp	↓Kp
PS	↓Kp, ↑Ki	stable	stable	stable	↓Kp, ↑Ki	↑Kp, ↑Ki	↑Kp, ↑Ki, slight ↓Kd
PM	↓Kp, ↑Ki, ↑Kd	↓Kp, ↑Ki	stable	↓Kp	↑Ki	↑Kp, ↑Ki	↑Kp, ↑Ki, ↑Kd
PB	moderate ↓Kp, ↑Kd	↓Kp, ↑Ki	↓Kp	↓Kp	↑Ki, ↓Kd	↑Kp, ↓Ki	↑↑Kp, ↓Ki, ↑↑Kd

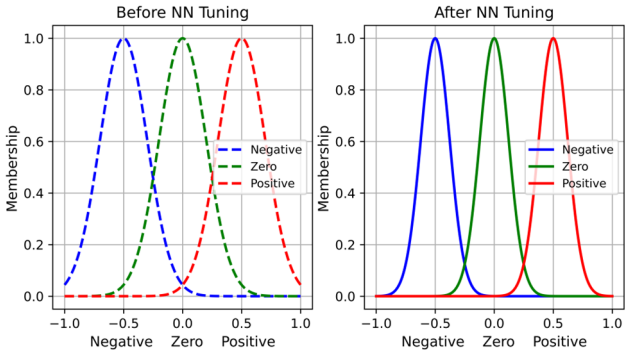

Fig. 9. Membership functions before and after NN tuning.

NB = Negative Big, NM = Negative Medium, NS = Negative Small, Z = Zero, PS = Positive Small, PM = Positive Medium, PB = Positive Big. Each entry specifies the corrective adjustments to PID gains K_p, K_i, K_d based on the combination of error e and error change Δe.

In the proposed NN-Fuzzy-PID framework, the neural network does not alter the structure of the fuzzy inference system or the predefined rule base. Instead, it adaptively tunes the parameters of the fuzzy membership functions to improve control performance under different operating conditions. Specifically, the neural network shifts the centers and scales the widths of the membership functions for the input variables, while preserving their original shapes. This approach preserves the interpretability of the fuzzy rules and prevents sudden changes in control behavior. Fig. 9 shows the membership functions before and after neural network tuning, illustrating the smooth and bounded adaptation process.

E. Neural Network-Based Online Adaptation and Stability Considerations

For the NN-Fuzzy-PID controller to adapt in real time, its neural network architecture, learning mechanism, and

update strategy must be clearly defined. Input-output variables, the online learning scheme, and computational parameters directly influence the controller's responsiveness, stability, and real-time performance. The neural network configuration used in this study is summarized below.

- Input: [e, $\dot{e}$, Δe, v, μ, load].
- Output: $\Delta K_p, \Delta K_i, \Delta K_d$].
- Loss function: defined in Eq. (11).
- Online learning.
- Learning rate: η.
- Sampling time Ts = 0.01s.

Both loops are implemented in Simulink and connected to the Simscape Multibody vehicle model. The fuzzy logic layer provides interpretable rule-based adjustments, while the neural network optimizes rule weights and membership functions online by minimizing a performance cost as Eq. (11):

$$J = \alpha e_\delta^2 + \beta e_\delta^2 + \lambda(\Delta K)^2 \quad (11)$$

where: J is designed to balance trajectory-tracking accuracy, steering smoothness, and control effort; αe_δ^2 penalizes the lateral tracking error to improve trajectory-tracking accuracy; βe_δ^2 penalizes steering-angle error to reduce oscillations and improve directional stability; and $\lambda(\Delta K)^2$ a regularization term limits gain variations to ensure smooth and robust control adaptation.

IV. Simulation Results

In a study, a series of simulation experiments was carried out in MATLAB/Simulink to evaluate the effectiveness of the proposed NN-Fuzzy-PID control framework. The simulations aimed to verify the controller's capability in trajectory tracking, velocity regulation, disturbance rejection, and robustness under nonlinear vehicle dynamics. For this purpose, a high-fidelity Ackermann-type autonomous vehicle model was developed in Simscape Multibody, allowing the integration of realistic steering kinematics, tire-road interactions, and inertial effects. The simulation setup and controller configurations are described below.

A. Simulation Setup

To evaluate the effectiveness of the proposed NN-Fuzzy-PID control framework, a series of simulation experiments was carried out in MATLAB/Simulink. The simulations aimed to verify the controller's capability in trajectory tracking, velocity regulation, disturbance rejection, and robustness under nonlinear vehicle dynamics. For this purpose, a high-fidelity Ackermann-type autonomous vehicle model was developed in Simscape Multibody, allowing the integration of realistic steering kinematics, tire-road interactions, and inertial effects.

The main parameters considered in the simulations include a vehicle mass of 1200 kg, a wheelbase of 2.6 m, a track width of 1.5 m, a maximum steering angle of ±30°, a maximum velocity of 25 m/s, and a sampling time of 0.01 s. Three controllers were benchmarked for comparison: a baseline PID, a Fuzzy-PID, and the proposed NN-Fuzzy-PID. The neural network was designed as a three-layer perceptron with a 5–10–3 structure, using ReLU activation in the hidden layer and linear outputs corresponding to the gain update $\Delta K_p, \Delta K_i, \Delta K_d$.

These parameters are selected based on typical mid-size passenger vehicle specifications reported in the literature, ensuring a realistic representation of vehicle dynamics and enabling fair comparison with existing studies.

B. Simulation Scenarios

The vehicle follows a reference trajectory composed of straight and curved road segments at constant velocity. This scenario evaluates baseline lateral tracking accuracy.

1) Scenario 2: Velocity regulation under varying loads

Step changes in the reference velocity are applied while the payload mass is varied by ±20%. This tests the longitudinal loop's ability to maintain stability and to minimize overshoot under load variations.

2) Scenario 3: Disturbance rejection

External disturbances are introduced, including lateral crosswinds of 300 N and slope-induced forces. The objective is to evaluate the controller's robustness in maintaining stable yaw and steering performance.

3) Scenario 4: Robustness under nonlinearities and uncertainties

The tire-road friction coefficient is varied between 0.4 and 0.9 to represent wet and dry road conditions. This scenario assesses the adaptability of the NN-Fuzzy-PID controller to parameter uncertainties and nonlinear dynamics.

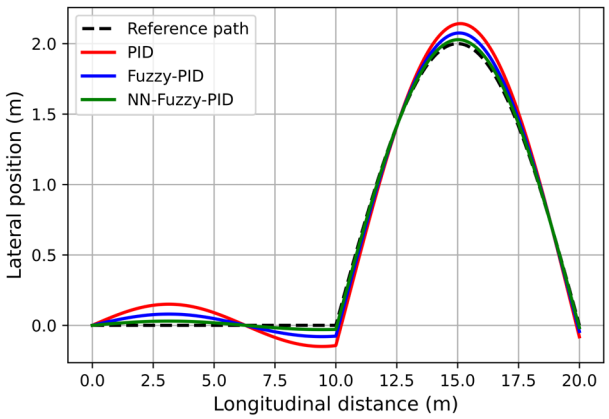

Fig. 10. Path tracking performance under nominal conditions: comparison of PID, Fuzzy-PID, and NN-Fuzzy-PID controllers.

C. Scenario 1: Path Tracking under Nominal Conditions

As seen in Scenario 1, the vehicle followed a reference trajectory that combined a straight and a curved path at a constant speed of 15 m/s to assess lateral accuracy. The tracking performance of the three controllers is represented in Fig. 10, and the quantitative results are presented in Table III. The baseline PID produced the largest error (RMSE: 0.25 m) and the peak deviation (RPD): >0.30 m;

the Fuzzy-PID had an RMSE of 0.18 m, and the peak deviation of approximately 0.20 m. The proposed NN-Fuzzy-PID achieved the lowest RMSE of 0.10 m and a peak deviation of <0.15 m, with an overall smoother steering correction. These results confirm the excellent performance of the NN-Fuzzy-PID controller over conventional PID and Fuzzy-PID, namely its accuracy and stability.

TABLE III. LATERAL TRACKING PERFORMANCE UNDER NOMINAL CONDITIONS (SCENARIO 1)

Controller	RMSE (m)	Peak Deviation (m)
PID	0.25	> 0.30
Fuzzy-PID	0.18	≈ 0.20
NN-Fuzzy-PID	0.10	< 0.15

D. *Scenario 2: Velocity Control under Varying Load Conditions*

In Scenario 2, the vehicle was required to maintain a constant velocity of 15 m/s under varying load conditions to evaluate longitudinal control performance. Fig. 11 illustrates the velocity-tracking results, and the quantitative metrics are summarized in Table IV. The baseline PID exhibited noticeable oscillations and slow recovery upon introduction of a load disturbance, with an RMSE of 0.42 m/s and an overshoot exceeding 8%. The Fuzzy-PID improved disturbance rejection, reducing RMSE to 0.28 m/s and limiting overshoot to around 5%. Notably, the proposed NN-Fuzzy-PID achieved the most stable performance, producing a minimum RMSE of 0.15 m/s, an overshoot below 3%, and a significantly shorter settling time than the conventional PID and Fuzzy-PID controllers. The NN-Fuzzy-PID controller has been shown to perform well in velocity regulation under nonlinear and uncertain operating conditions, outperforming PID and Fuzzy-PID controllers.

E. *Scenario 3: Disturbance Rejection—Crosswind and Slope*

In these cases, the vehicle experiences external disturbances, including a lateral crosswind of 300 N and slope-induced forces, while following a reference trajectory of 15 m/s, to ensure the controllers' stability and robustness under sudden shocks. Fig. 12 shows lateral deviation responses to disturbances, while Table V summarizes the quantitative results. The baseline PID showed considerable oscillations, with the lateral deviation reaching a maximum of 0.45 m, and it took more than 6.0 s to stabilize. The Fuzzy-PID controller improved stability, with a maximum deviation of 0.28 m and a recovery time of around 4.1 s. The proposed NN-Fuzzy-PID exhibited great robustness, with a maximum range of only 0.15 m and a recovery time under 2.5 s, yet its correction rates remained smoother than those of the other two. We conclude that the NN-Fuzzy-PID controller can successfully reject disturbances, as evidenced by its rapid recovery, and significantly outperforms both conventional PID and Fuzzy-PID. Its flexibility enables it to maintain precise control under a wide range of external conditions.

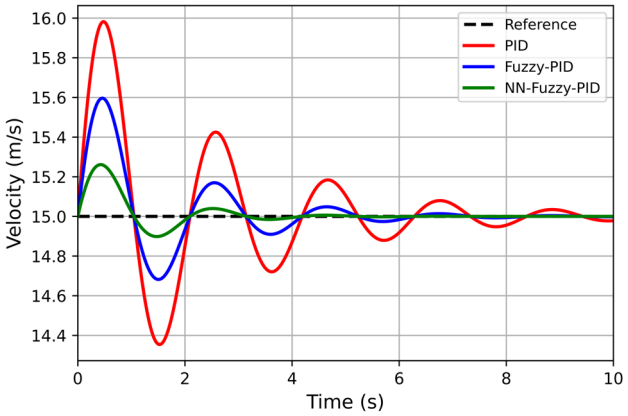

Fig. 11. Regulation performance under load disturbance for PID, Fuzzy-PID, and NN-Fuzzy-PID controllers.

TABLE IV. QUANTITATIVE PERFORMANCE COMPARISON OF PID, FUZZY-PID, AND NN-FUZZY-PID CONTROLLERS IN SCENARIO 2

Controller	RMSE (m/s)	Overshoot (%)	Settling time (s)
PID	0.42	8.2	5.2
Fuzzy-PID	0.28	5.1	3.8
NN-Fuzzy-PID	0.15	2.7	2.4

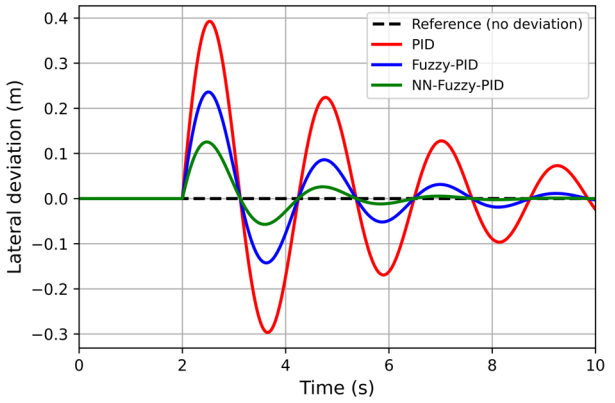

Fig. 12. Lateral deviation responses under crosswind disturbance (300 N) and slope effects for PID, Fuzzy-PID, and NN-Fuzzy-PID controllers.

TABLE V. DISTURBANCE REJECTION PERFORMANCE UNDER CROSSWIND AND SLOPE CONDITIONS

Controller	Max deviation (m)	Recovery time (s)	Oscillation amplitude (°)
PID	0.45	6.0	9.2
Fuzzy-PID	0.28	4.1	5.3
NN-Fuzzy-PID	0.15	2.5	2.7

F. *Scenario 4: Robustness under Nonlinearities and Uncertainties*

In this picture, the vehicle ran in different road—tire friction coefficients ranging from 0.4 (wet road) to 0.9 (dry road) while exhibiting a curved trajectory at 15 m/s, a range that aimed to make the controller more robust to nonlinear dynamics and parameter uncertainties. Fig. 13 contains the lateral variation across different friction levels; Table VI provides quantitative metric summaries. The results in Fig. 13 clearly show that the PID controller's performance significantly deteriorated under low-friction conditions (μ = 0.4), indicating oscillatory behavior. On the other hand, the NN-Fuzzy-PID converges well and

demonstrates low lateral deviation. This validates the robustness of the adaptive gain mechanism under parameter uncertainty. The baseline PID performance was substantially worse on low-friction surfaces, with RMSE rising to 0.48 m and frequent instability. Adaptation was further enhanced using this Fuzzy-PID parameter, which limited RMSE to 0.31 m only, but was still prone to oscillation when friction slipped below the threshold of 0.5. The developed NN-Fuzzy-PID proved more robust, showing a lower RMSE (RMSE < 0.18 m) at all friction conditions with steady convergence. These results may indicate that PID and Fuzzy-PID controllers are sensitive to parameter variations, whereas the NN-Fuzzy-PID adapts to fluctuating road conditions, enabling consistent and reliable performance.

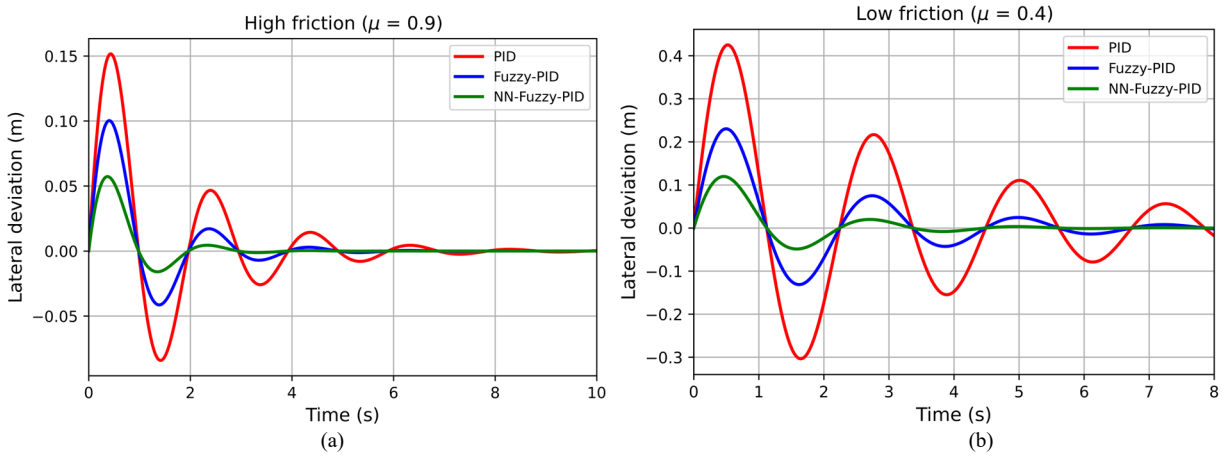

Fig. 13. Lateral deviation under varying tire-road friction conditions: (a) High friction (μ = 0.9); (b) Low friction (μ = 0.4).

TABLE VI. ROBUSTNESS TO VARYING TIRE-ROAD FRICTION COEFFICIENTS (M = 0.4–0.9)

Controller	RMSE (μ = 0.9) (m)	RMSE (μ = 0.4) (m)	Stability under low μ
PID	0.22	0.48	Marginal (oscillatory)
Fuzzy-PID	0.19	0.31	Stable but oscillatory
NN-Fuzzy-PID	0.12 m	0.18 m	Stable and smooth

To provide an overall quantitative comparison, Table VII summarizes the percentage improvements achieved by the proposed NN-Fuzzy-PID controller over the baseline PID and Fuzzy-PID controllers across all evaluated scenarios.

The neural network is trained using simulation data collected under varying friction levels, vehicle loads, and trajectory curvatures. The dataset is divided into training and validation sets, and the loss function weights are selected to balance tracking accuracy and control smoothness.

TABLE VII. SUMMARY OF PERFORMANCE IMPROVEMENTS OF NN-FUZZY-PID COMPARED WITH PID AND FUZZY-PID

Performance metric	PID	Fuzzy-PID	NN-Fuzzy-PID	Improvement vs. PID (%)	Improvement vs. Fuzzy-PID (%)
Lateral RMSE (m)	0.25	0.18	0.10	↓ 60.0	↓ 44.4
Peak lateral deviation (m)	>0.30	≈ 0.20	<0.15	↓ ≈ 50.0	↓ ≈ 25.0
Velocity RMSE (m/s)	0.42	0.28	0.15	↓ 64.3	↓ 46.4
Overshoot (%)	8.2	5.1	2.7	↓ 67.1	↓ 47.1
Settling time (s)	5.2	3.8	2.4	↓ 53.8	↓ 36.8
Disturbance recovery time (s)	6.0	4.1	2.5	↓ 58.3	↓ 39.0
RMSE under low friction (μ = 0.4) (m)	0.48	0.31	0.18	↓ 62.5	↓ 41.9

G. Controller Failure Conditions and Robustness Mechanism

Conventional PID control degrades significantly under low-friction conditions (μ < 0.5), high-curvature trajectories, or sudden load variations, due to its fixed-gain structure. Similarly, fixed-rule Fuzzy-PID controllers may exhibit oscillatory behavior when operating conditions deviate from the tuning region of predefined membership functions.

In contrast, the proposed NN-Fuzzy-PID controller mitigates these limitations through online adaptation. The neural network continuously adjusts the fuzzy membership centers and PID gains in response to variations in tracking error, velocity, and estimated friction. As observed in Scenario 4, while PID becomes marginally stable under μ = 0.4, the NN-Fuzzy-PID maintains bounded RMSE (<0.18 m) and smooth convergence.

This adaptive mechanism allows the controller to compensate for parameter uncertainty and nonlinear tire dynamics without manual retuning.

V. DISCUSSION

The simulation results demonstrate that the proposed NN-Fuzzy-PID controller effectively improves trajectory tracking and velocity regulation for Ackermann-type autonomous vehicles under nonlinear dynamics and

uncertain operating conditions. The observed performance gains can be attributed to online neural network–based adaptation of fuzzy membership functions and PID gains, enabling the controller to respond promptly to variations in road friction, vehicle load, and external disturbances without manual retuning.

Compared with conventional PID and fixed-rule Fuzzy-PID controllers, the proposed approach offers a balanced trade-off between adaptability and interpretability. While advanced model-based controllers such as MPC and sliding-mode control provide strong robustness, their computational complexity and dependence on accurate system models limit their applicability to low-cost embedded platforms. In contrast, the NN-Fuzzy-PID controller achieves comparable robustness with significantly lower computational overhead, making it more suitable for real-time autonomous driving applications.

From a practical implementation perspective, the average computation time below 1 ms per control step confirms that the proposed controller can be deployed on resource-constrained embedded hardware commonly used in automotive systems. The use of a lightweight neural network and bounded online updates ensure stable operation without excessive processing demands. However, the current study is limited to simulation-based validation using a Simscape Multibody model, and it does not provide formal stability guarantees for the neural network adaptation mechanism. Future work will therefore focus on hardware-in-the-loop testing and real-vehicle experiments, as well as on extending the stability analysis to more rigorous theoretical frameworks.

Conventional PID control tends to reduce performance under low-friction conditions or sudden load changes because its fixed-gain structure cannot adapt. Fixed-rule Fuzzy-PID controllers may also show oscillations when operating outside their set tuning region. The proposed NN-Fuzzy-PID overcomes these issues by continuously adjusting membership functions and PID gains in real time, enabling the controller to maintain stable tracking performance across different road-tire conditions.

While the simulation results are promising, practical implementation may introduce challenges such as sensor noise, actuator saturation, and computational delays. These factors will be addressed in future hardware-in-the-loop and real-vehicle experiments through appropriate filtering, anti-windup strategies, and bounded adaptation mechanisms.

The Simscape Multibody model and controller configuration used in this study will be made available upon reasonable request to support reproducibility and further research.

VI. Conclusion

This paper presents and extensively simulates a neural network-based control system for Ackermann-type self-driving cars. Even in situations with nonlinear dynamics, disturbances, and uncertain road and tyre conditions, the proposed dual-loop NN-Fuzzy-PID controller efficiently enhances steering and speed control. This method greatly reduces tracking errors, overshoots, and settling times while remaining affordable for real-time use, according to simulation results from four scenarios, compared with regular PID and fuzzy-PID controllers. This study uses a simple tyre model for simulation-based validation. Future research will focus on extending the framework to real-vehicle experiments and hardware-in-the-loop testing, as well as on investigating performance under more demanding driving conditions and formal stability guarantees. Subsequent research will focus on extended stability analysis and experimental validation under more demanding driving conditions.

Conflicts of Interest

The authors declare no conflict of interest.

Author Contributions

Conceptualization, Methodology, Formal analysis, Software, Writing, T.H.V.; Validation, Investigation, Resources, Data curation, T.T.C. and Q.V.V.; Review and editing, Supervision, Project administration, H.Q.N.; all authors had approved the final version.

Acknowledgment

The authors gratefully acknowledge Thai Nguyen University of Technology, Vietnam, for its support of this work.

References

[1] A. Sahoo and S. K. Dwivedy, "Adaptive fuzzy PID controller for a compact autonomous underwater vehicle," in *Proc. Global Oceans 2020: Singapore–U.S. Gulf Coast*, Singapore, 2020, pp. 1–6. doi: 10.1109/IEEECONF38699.2020.9389483

[2] Y. Sun, X. Liu, J. Zhang *et al.,* "Neural-network-based adaptive MPC path tracking control for 4WID vehicles using phase plane analysis," *Applied Sciences,* vol. 15, no. 19, 10598, 2025. doi: 10.3390/app151910598

[3] D. Xu, G. Wang, L. Qu *et al.,* "Robust control with uncertain disturbances for vehicle drift motions," *Applied Sciences,* vol. 11, no. 11, 4917, 2021. doi: 10.3390/app11114917

[4] M. S. Albhaisi, M. Prauzek, T. T. H. Minh *et al.,* "Trajectory tracking control for autonomous vehicles: A systematic PRISMA review of models and strategies," *Annual Reviews in Control,* vol. 61, 101047, 2026. doi: 10.1016/j.arcontrol.2026.101047

[5] J. Lee and S. Yim, "Comparative study of path tracking controllers on low friction roads for autonomous vehicles," *Machines,* vol. 11, no. 3, 403, 2023. doi: 10.3390/machines11030403

[6] J. Ito and Y. Wasa, "Data-driven adaptive PID control based on physics-informed neural networks," arXiv preprint arXiv: 2510.04591, 2025. doi: 10.48550/arXiv.2510.04591

[7] R. Alika, E. M. Mellouli, and E. H. Tissir, "A modified sliding mode controller based on fuzzy logic to control the longitudinal dynamics of the autonomous vehicle," *Results in Engineering*, vol. 22, 102120, 2024. doi: 10.1016/j.rineng.2024.102120

[8] T. H. Vo, M. H. Nguyen, H. V. Tran *et al.,* "Experimental study on navigation control of autonomous vehicles using a predictive control model," *SSRG Int. J. Electr. Electron. Eng.,* vol. 11, no. 5, pp. 235–241, 2024. doi: 10.14445/23488379/IJEEE-V11I5P121

[9] D. Kapsalis, O. Sename, V. Milanés *et al.,* "Gain-scheduled steering control for autonomous vehicles," *IET Control Theory & Applications*, vol. 14, no. 20, pp. 3451–3460, 2020. doi: 10.1049/iet-cta.2020.0698

[10] Z. Han, J. Ruan, J. Hu *et al.,* "Deep reinforcement learning based adaptive trajectory tracking control strategy for four-wheel independent steering vehicles," *Neurocomputing,* vol. 685, 133649, 2026. doi: 10.1016/j.neucom.2026.133649

[11] G. Ahmad, M. Zaery, M. Shafiullah *et al.,* "Hardware-in-the-loop validation of the optimized controller for stabilizing islanded microgrids with cryptocurrency mining loads," *Renewable Energy Focus*, 100868, 2026. doi: 10.1016/j.ref.2026.100868

[12] Aliskan, "The optimization-based fuzzy logic controllers for autonomous ground vehicle path tracking," *Engineering Applications of Artificial Intelligence*, vol. 151, 110642, 2025. doi: 10.1016/j.engappai.2025.110642

[13] B. Li, D. Li, and F. Yu, "Vehicle yaw stability control using the fuzzy-logic controller," in *Proc. IEEE International Conf. on Vehicular Electronics and Safety (ICVES)*, Beijing, China, 2007, pp. 1–5. doi: 10.1109/ICVES.2007.4456392

[14] Boyali, S. Mita, and V. John, "A tutorial on autonomous vehicle steering controller design, simulation and implementation," arXiv preprint, arXiv: 1803.03758, 2018.

[15] M. Samuel, K. Yahya, H. Attar *et al.,* "Evaluating the performance of fuzzy-PID control for lane recognition and lane-keeping in vehicle simulations," *Electronics*, vol. 12, no. 3, 724, 2023. doi: 10.3390/electronics12030724

[16] M.-D. Duong, Q.-T. Pham, T.-C. Vu *et al.,* "Adaptive fuzzy sliding mode control of an actuator powered by two opposing pneumatic artificial muscles," *Scientific Reports*, vol. 13, 8242, 2023. doi: 10.1038/s41598-023-34491-3

[17] T.-V.-A. Nguyen, Q.-T. Dao, and N.-T. Bui, "Optimized fuzzy logic and sliding mode control for stability and disturbance rejection in rotary inverted pendulum," *Scientific Reports*, vol. 14, 31116, 2024. doi: 10.1038/s41598-024-82471-y